J Solid State Electrochem (2006) 10: 458–464
DOI 10.1007/s10008-005-0015-9

ORIGINAL PAPER

Renáta Oriňáková · Hans-Dieter Wiemhöfer
Jürgen Paulsdorf · Veronika Barinková
Anna Bednáriková · Roger M. Smith

Impedance study of Ni–Co electro-deposition on Fe powder particles in fluidised bed systems

Received: 28 September 2004 / Revised: 15 February 2005 / Accepted: 16 February 2005 / Published online: 26 July 2005

Abstract The electrochemical impedance method was applied during the electrochemical deposition of a binary Ni–Co coating on iron powder in a fluidised bed electrode system. The influence of the suspension density on the charge transfer in the course of the electro-deposition process was studied. At a potential of −900 mV (vs. Ag/AgCl/3 M KCl), when the binary Ni–Co layer was formed, the impedance data were characterised by two semicircles with the semicircle at high frequencies being larger in magnitude. A contribution of the diffusion process to the overall current was observed. The optimal suspension density for the charge transfer in the bed was 10×10^{-3}–15×10^{-3} (i.e., 4–6 g of iron powder in 50 ml of electrolyte). The most probable mechanism of the charge transfer for the studied concentrations of powder particles is the convective mechanism. The iron particles dispersed in the electrolyte were considered to act as either a depolariser or an additional working electrode depending on the applied electrode potential and on the suspension density.

Keywords ElS · Electro-deposition · Ni–Co · Charge transfer · Fluidised bed electrode · Iron microparticles

R. Oriňáková (✉) · V. Barinková · A. Bednáriková
Institute of Chemistry, P.J. Šafárik University, 04101 Košice, Slovak Republic
E-mail: orinako@kosice.upjs.sk
Tel.: +421-55-6222605
Fax: +421-55-6222124

H.-D. Wiemhöfer · J. Paulsdorf
Institute of Inorganic and Analytical Chemistry, University of Münster, 48149 Münster, Germany

R. M. Smith
Department of Chemistry, Loughborough University, LE11 3TU, Loughborough, UK

Introduction

A fluidised bed electrode consists of solid metallised or metallic particles, dispersed by a vertical flow of electrolyte [1] or by a stirring of the electrolyte solution [2]. The dispersed particles intermittently come into contact with the solid electrode to be charged and are thereby plated with a metallic layer. The main advantages of the fluidised bed electrode are a significant increase of the active surface to volume ratio and a strongly enhanced material transport. Several authors have studied and modelled details of the charge transport [3–6] and mass transfer in systems with vertical electrolyte flows [7, 8]. The electronic conduction within the fluidised bed electrode has also been discussed and different mechanisms have been proposed. The convective transport of charged particles accompanied by charge sharing collisions with other particles is the most frequently accepted explanation for the enhanced electron transport [5, 9]. An alternative mechanism of conduction through chains and aggregates of particles, i.e., the so-called conductive mechanism, is also well developed, but requires a very high number of collisions [5, 10]. A bipolar mechanism was introduced to explain the deviations from the proposed behaviour according to the convective and conductive mechanisms [5]. A further quantitative model describing fluidised bed electrodes with a circular movement of the suspension has also been developed [11] and extended [12, 13]. However, detailed experimental studies of the charge transport in these systems are still in their infancy and they have to be extended yet [14].

A fluidised bed electrolyser was first described in 1966 and a few routine applications can be found, for example, in fuel cells, organic electrosynthesis and metal electrowinning from very dilute solutions [7]. Recently, the use of fluidised bed electrolysis has expanded [15, 16] and a popular application of fluidised bed reactors is the removal and recovery of heavy metals from aqueous solutions by bio-sorption and electrolysis [17, 18].

The electrolytic plating of metallic layers onto conducting micro- and nanoparticles is a new application of the fluidised bed electrode and has been used for the refinement of the basic material properties in powder metallurgy. Coatings deposited in this way are of good-quality, uniform and adherent. Moreover electrochemical techniques provide a high level of control. After 30 min of electrolysis with an applied current of 1 A, the coating layer thickness varied from 5 μm to 10 μm depending on the other conditions. There is a wide field of applications for such particles, most notably in electronics, powder metallurgy, aerospace, medicine and pharmacy. We believe that the deposition of thin metallic or polymeric films on particles in fluidised bed is a forthcoming technique for catalysis, waste-water cleaning and nanoscience.

Until now, the problem of alloying different metals in powder metallurgy was mainly solved either by mechanical mixing of powders or by their melting and mixing. Although, in most cases, these procedures provide a sufficiently homogeneous product, they failed when the metals to be mixed considerably differed in their densities or showed a tendency for the segregation of the components. The electrochemical deposition of a metal film on a primary powder may result in a more favourable product. In general, the quality of an electrochemical coating depends primarily on the efficient transfer and distribution of charge in a fluidised bed electrode. In the optimal case, every particle of the powder will be coated by the plating metal(s) thus ensuring a high homogeneity of the final product.

There is still great interest in the electro-deposition of the iron-group metals, because of their important mechanical and magnetic properties, which offer many industrial applications, e.g., in microsystem technologies of sensors and actuators, in rocket technology, astronautics, for anticorrosive coatings, and for decorative purposes [19, 20, 21]. For example, the presence of cobalt in nickel alloys is known to improve the hardness of the solids.

The electroplating of Ni–Co alloys has been recognised as an anomalous co-deposition and is characterised by a preferential deposition of the less noble metal Co [22], even when the concentration of Ni in the bath was higher than that of Co [22, 23, 24]. The efficiency of the electrolytic coating of powdered material is strongly affected by the applied current density, the rotation speed, the average size of the particles and the density of the electrolyte-powder suspension. The present work investigates the influence of the suspension density on the electroplating of dispersed powder materials with binary Ni–Co coatings. The impedance of the fluidised bed electrode was measured during the electrolytic deposition to study the charge transfer between the surface of the solid cathode and the powder particles in the vicinity of the electrode and in the fluidised bed electrode and to understand in detail the electroplating of powdered material.

Experimental

Materials

Iron powder prepared by a pressure water atomisation process (Mannesmann) was used as the standard material for electrolytic coating. The granulometric class of iron powder used in every experiment was in the range of 0.063–0.100 mm. The specific surface area of Fe powder was measured by the BET method using nitrogen gas.

Method

The polarisation curves were recorded using a potentiostat (PerkinElmer, model 283). The working electrode was polarised in the potential range $0\,V \div -1.5\,V \div +1.5\,V \div 0\,V$ (vs. Ag/AgCl/3 M KCl). The corresponding electrochemical cell with three electrodes is shown in Fig. 1.

The working electrode was a paraffin-impregnated graphite electrode (PIGE) embedded in an insulating epoxy resin. The contact surface with the solution was circular with an area of 0.283 cm^2 . The working electrode was cleaned with emery paper and polished by glossy paper before starting a measurement. The counter and reference electrodes were made of Pt (with an area 8.79 cm^2) and Ag/AgCl with 3 M KCl solution (Schott-Geräte GmbH), respectively. The Pt electrode was thoroughly cleaned in nitric acid (1:1) and rinsed with distilled water before use. The electrolyte solution was a mixture of 0.69 mol/L $NiSO_4$, 0.125 mol/L $CoSO_4$ and 0.26 mol/L NaCl, adjusted to pH = 2 with diluted H_2SO_4 solution.

The electrochemical impedance was measured by using a potentiostat/galvanostat (Perkin-Elmer, model 283) and a frequency response analyser (Solartron, SI 1260). The experimental data were analysed using the Zplot software package (Scribner Ass.). The amplitude

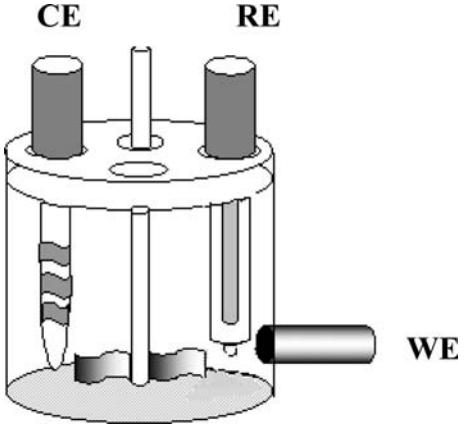

Fig. 1 Scheme of the experimental fluidised bed arrangement used for EIS measurements. *WE* working electrode (PIGE); *RE* reference electrode (Ag/AgCl); *CE* counter electrode (Pt)

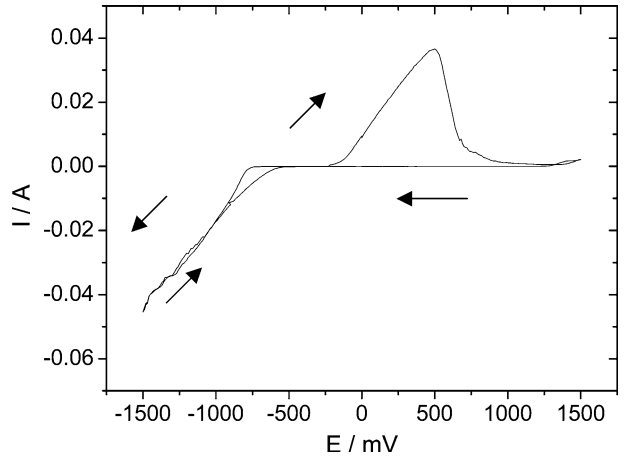

Fig. 2 Polarisation curve for binary alloy (Ni–Co) electro-deposition on PIGE performed in electrolyte: 0.69 mol/L $NiSO_4$, 0.125 mol/L $CoSO_4$ and 0.26 mol/L NaCl (pH = 2) with scan rate 100 mV/s, in the potential range 0 V ÷ −1.5 V ÷ +1.5 V ÷ 0 V (vs. Ag/AgCl/3 M KCl). Solution was not bubbled with N_2

of the imposed potential modulation was 500 mV. This was necessary to reach a good signal-to-noise ratio. It was checked that the basic impedance characteristics was still linear, i.e., the impedance should have no dependence on the chosen voltage amplitude (amplitudes of 20–50 mV are usually applied to prevent non-linear contributions). The open circuit cell voltage was taken as the DC voltage. Thus, the DC currents were 0.1 mA and lower. The chosen frequency range was from 1 MHz to 0.1 Hz. The electrochemical cell and the electrodes were the same as for the polarisation measurements (e.g. Fig. 1).

The relative suspension density is described by the volume fraction ϕ of the suspended particles (in percent) and was defined as the percentage of the volume of the solid particles (Fe powder) in the suspension (V_p) with respect to the total volume of the electrolyte solution and the suspended particles according to

$$\phi_{susp}[\%] = 100V_p/(V_{el} + V_p), \quad (1)$$

V_{el} is the volume of the liquid electrolyte, and V_p is the volume of the suspended solid particles. In our experiments, volume fractions between 0.50% and 3% were employed (Table 1).

Table 1 The values of suspended particles volume fraction ϕ_{susp} and surface area calculated for different amounts of Fe powder in 50 ml of electrolyte

Mass of Fe powder in 50 ml of electrolyte (g)	Volume of Fe powder (cm^3)	Surface area of Fe powder (cm^2)	Volume fraction of suspended particles ϕ_{susp} (%)
2	0.25	438	0.50
4	0.51	876	1.01
6	0.76	1 314	1.50
8	1.02	1 752	2.00
10	1.27	2 190	2.48
12	1.52	2 628	2.95

Results and discussion

Electrode reactions during electro-deposition of Ni and Co on Fe surfaces

Studies of the elemental electrochemical depositions of Ni and Co have indicated that the metal monohydroxide, $MeOH^+$, is an important species in the charge-transfer steps [25]. The reaction pathway as discussed by Bockris [26] is assumed here for the electrolytic deposition of all iron-group metals and alloys:

$$Me^{2+} + H_2O \Longleftrightarrow MeOH^+_{aq} + H^+ \quad (2a)$$

$$MeOH^+_{aq} \Longleftrightarrow MeOH^+_{ads} \quad (2b)$$

$$MeOH^+_{ads} + e^- \rightarrow MeOH \quad (3)$$

$$MeOH + H^+ + e^- \rightarrow Me + H_2O \quad (4)$$

where Me stands for Co and Ni atoms and $MeOH^+_{ads}$ denotes an adsorbed species. The rate-determining step (rds) can switch from Eq. 3 to Eq. 4 as the cathodic potential becomes more negative. Some studies also proposed the participation of other anions such as Cl^- and SO_4^{2-} in the electrodeposition mechanism [27].

The deposition of Ni–Co also implies that the reduction of Me^{2+} ions is accompanied by hydrogen adsorption. This is the first step leading to hydrogen evolution on the surface of the deposited layer, which is also a complex multistep reaction [28]:

$$Me + H^+ + e^- \rightarrow Me - H_{ads} \quad (5)$$

$$2Me - H_{ads} \rightarrow 2Me + H_2 \quad (6a)$$

$$Me - H_{ads} + H^+ + e^- \rightarrow Me + H_2 \quad (6b)$$

The polarisation curve for a binary alloy deposited on PIGE is presented in Fig. 2. The cathodic part of the curve reflects a reduction of metallic ions on the working PIGE surface. It is characterised by an increase in the current, below the deposition potential (−800 mV).

The anodic part of the polarisation curve corresponds to the dissolution of the metallic layer deposited on PIGE during the preceding cathodic process. The occurrence of a single oxidation peak indicates that the dissolution of the two metals in the binary alloy progresses either simultaneously, or at very similar potentials.

Expected impedance in the presence of dispersed metal microparticles

The impedance of a fluidised bed electrode is a fluctuating quantity if we assume a continuous stirring of the electrolyte. The short intermediate contacts of the suspended single microparticles with the electrode occur

randomly and thus modulate the effective cathode surface area and hence the impedance. Each encounter of a particle (i.e. its electrical contact to the cathode for a short time period Δt) can be expected to yield a current pulse. The time dependence of the pulse should be determined by the capacitive component for the charging of the double layer between particle and surrounding solution. After complete charging of the double layer, a cathodic reaction can start, if the applied potential at the cathode is sufficient. This single contact event will be restricted to a very short time period (due to the stirring) so that no significant concentration polarisation can occur. The latter is one of the main advantages of the fluidised bed concept.

The total current, therefore, is principally the sum of delta-like current pulses from single particle contacts and the working graphite electrode current. The frequency dependence of the impedance will include a medium to high frequency component, which is determined by the stirring frequency, the suspension particle density, and the flow pattern of the electrolyte solution. An estimation gives a value for the maximum contact time interval of less than 1–10 ms for single particles at the cathode for a stirring frequency of 1 to 10 Hz. This value should lead to a maximum of the noise component in the impedance spectrum near 1 kHz and higher. This agrees well with an observed strong noise influence at impedance measuring frequencies higher than 1 kHz. The study therefore used an extended integration time for the impedance measurement at each frequency in order to eliminate the fluctuations from the high frequency noise and the results therefore correspond to an averaged low frequency impedance below 1 kHz.

The electrolyte solutions examined had high concentrations and will contribute a frequency-independent series resistance R_S, between 1 Ω and 15 Ω (calculated for the applied cell geometry). The bulk capacitance of the electrolyte can be neglected at the frequencies under study. The averaged electrode impedance at the interface of the fluidised bed electrode should therefore be the only frequency-dependent contribution. To a first-order approximation, it should represent a capacitive component and, if the applied potential is sufficient and an electrode reaction can occur, with a charge-transfer resistance in parallel. No substantial concentration polarisation and thus no large Warburg impedance is expected. The measured frequency dependence of the impedance should mainly reflect the properties of the interface cathode, plus an average number of interacting microparticles. The latter will depend on the suspension density.

The charge transport in the electrolyte solution is not expected to contain a significant contribution due to electron transport by the mutual contacts of the particles. The suspension density in our case (less than a volume fraction 3%) is small compared to the percolation threshold (the probability of continuous chains of contacting particles), which is at a volume fraction of 30%. The amount of charge which can be transmitted by moving polarised microparticles must also be negligible compared to the ion transport within the electrolyte solution.

Impedance results at 0 mV polarisation voltage

Figure 3 shows the impedance results for a potential of 0 V (vs. Ag/AgCl/3 M KCl). Under these conditions, no deposition of metallic layers can occur on the suspended microparticles. The effects of the changing suspension density on the magnitude (Fig. 3a) and phase (Fig. 3b) of the impedance are depicted. The results can be fitted by adopting the equivalent circuit shown in Fig. 4a with the electrolyte resistance R_S and the electrode impedance consisting of a capacitive constant phase element CPE and a charge-transfer resistance R_C. The impedance of the CPE is a function of two parameters: $Z_{CPE} = f(CPE\text{-}T, CPE\text{-}P)$, where $CPE\text{-}T$ is the ideal capacitance and

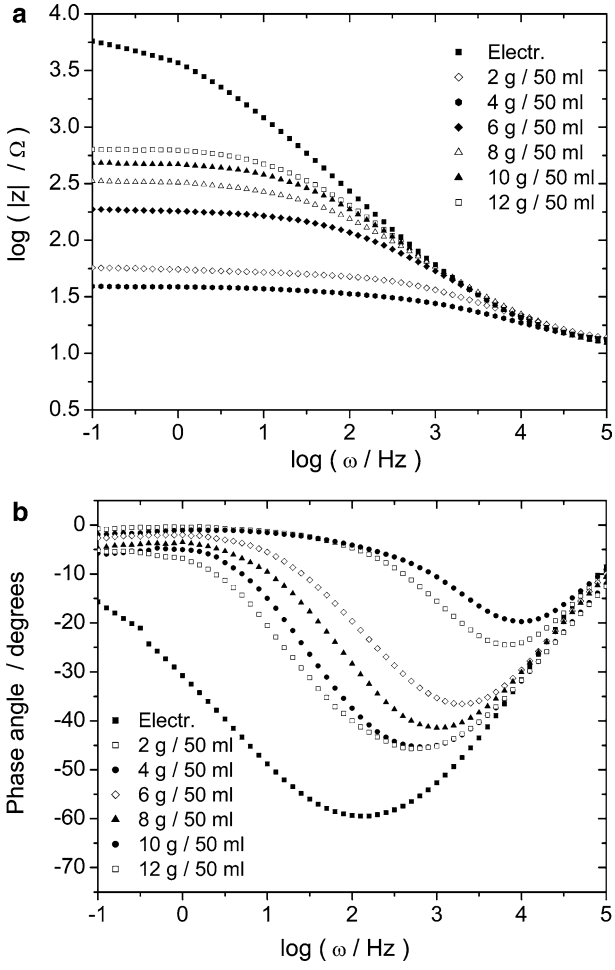

Fig. 3 Bode plots of the impedance data obtained at potential 0 V (vs. Ag/AgCl/3 M KCl). The solution consisted of: 0.69 mol/L $NiSO_4$, 0.125 mol/L $CoSO_4$ and 0.26 mol/L NaCl (pH = 2). Solution was not bubbled with N_2. **a** The logarithm of absolute impedance as a function of frequency logarithm. **b** The logarithm of phase shift as a function of frequency logarithm

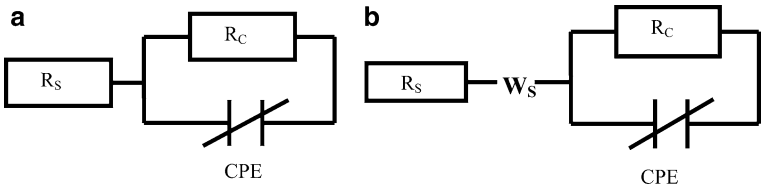

Fig. 4 Equivalent circuit used to fit the dates obtained for the fluidised bed electrode **a** at potential 0 V (vs. Ag/AgCl/3 M KCl); **b** at binary Ni-Co alloy deposition potential −900 mV (vs. Ag/AgCl/3 M KCl)

CPE-P is an empirical constant, $0 \leq CPE\text{-}P \leq 1$. Table 2 gives the fitted values and the experimental results. As expected, R_S is nearly constant. The constant phase element CPE is also nearly constant indicating that the particles do not significantly change the effective electrode area. However, R_C changes substantially. The initial value of R_C = 7,412 Ω corresponds to a spurious charge transfer (e.g. due to traces of adsorbed oxygen). The addition of 2 g/50 mL of Fe microparticles depolarises the cathode. This may be explained by a catalytic effect on the reaction of the adsorbed impurities. Increasing the suspension density leads to a strong increase of the charge-transfer resistance, R_C. The reason must be the limited quantity of adsorbed impurities, which are more effectively removed by the higher amount of particles. An alternative explanation is that the addition of solid iron particles to the electrolyte at a potential of 0 V represents the addition of a depolariser (electroactive substance). The dissolution (oxidation) of the particles in contact with the current feeder can occur, significantly lowering the charge-transfer resistance R_C. Apparently, only a small fraction of the added particles participates in the charge-transfer process. Increasing the suspension density leads to a weak increase in the number of iron particles involved in the charge transport and to a strong increase in the number of uncharged particles. The ratio of uncharged to charged particles increases with the suspension density, magnifying the charge-transfer resistance R_C. The increasing probability of multiple particle contacts at the electrode interface does not appear to be a decisive factor (if present it should lead to an increase of CPE and a decrease of R_C).

Impedance results at −900 mV polarisation voltage

In the potential range near −900 mV, where the binary nickel–cobalt alloy is deposited on PIGE as well on iron particles, the impedance plot exhibits a characteristic high-frequency behaviour, with a dominant superimposed noise above $\omega = 10^5$ Hz, as shown in the Nyquist plot (Fig. 5). The high-frequency behaviour is quite different in comparison to Fig. 3a and b, clearly indicating the presence of the deposition reaction modulated by the frequent brief particle contacts. Owing to a lack of suitable dynamic models, we cannot analyse this part of the frequency spectrum in detail. It should be possible with a model which takes into account the velocity of the solution moving along the electrode surface.

Figure 4b shows the equivalent circuit which we used to fit the observed results in Figs. 5 and 6. It is equivalent to the circuit in Fig. 4a, except that for the addition of a Warburg element in series. The analysis of the calculated values shows the following observations. The electrolyte resistance is low, nearly constant and independent on the suspension density. The charge-transfer resistance, R_C, decreases by factor of ten for the first two suspension densities and then slightly increases at a low rate. There seems to be an optimum for the charge transfer at a concentration of particles of 6 g in 50 mL, which is likely to be due to the convective mechanism. With a further increase in the suspension density, the amount of particles in the bed is getting rather high for the convective mechanism but it is still too low for another (conductive or bipolar) mechanism of charge transport. The charge-transfer resistance, R_C, is 100 to

Table 2 The values of resistances and constant phase element calculated from equivalent circuit model in Fig. 4a

Mass of Fe powder in 50 ml of electrolyte/ g	R_S/Ω	R_C/Ω	CPE-T×10^5/F	CPE-P
0	11.5	7412	3.82	0.71
2	11.4	11.4	2.67	0.72
4	10.2	27.6	7.80	0.63
6	11.2	169	4.48	0.68
8	11.2	315	4.98	0.67
10	10.1	491	4.45	0.69
12	10.1	692	4.86	0.68

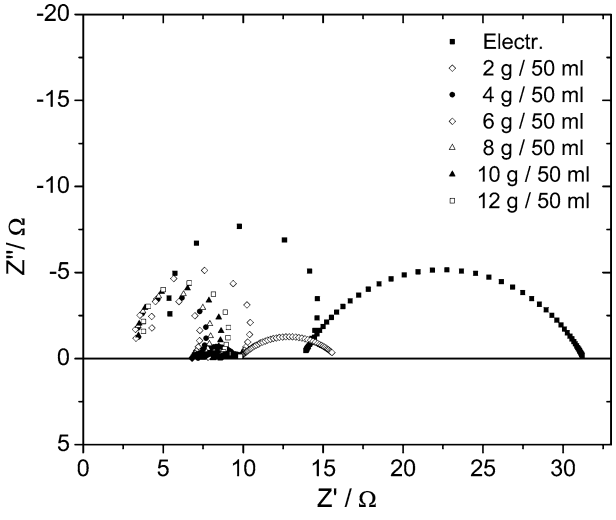

Fig. 5 Nyquist plots for the impedance data measured at the binary Ni–Co alloy deposition potential of −900 mV versus Ag/AgCl/3 M KCl. The solution consisted of 0.69 mol/L $NiSO_4$, 0.125 mol/L $CoSO_4$ and 0.26 mol/L NaCl (pH = 2). Solution was not bubbled with N_2

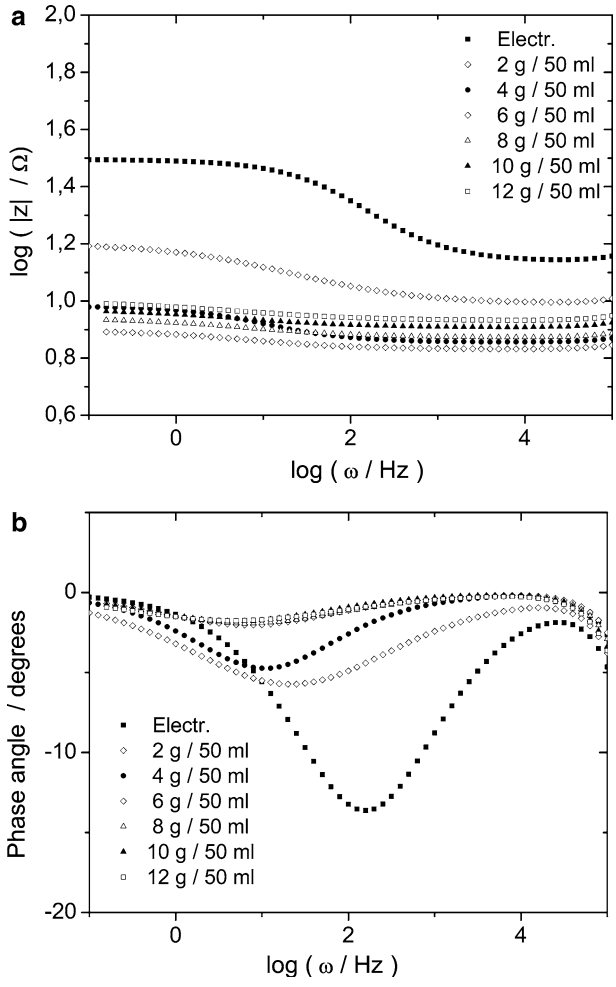

Fig. 6 Bode plots of the impedance data obtained at the binary Ni–Co alloy deposition potential −900 mV versus Ag/AgCl/3 M KCl. The solution consisted of 0.69 mol/L $NiSO_4$, 0.125 mol/L $CoSO_4$ and 0.26 mol/L NaCl (pH = 2). Solution was not bubbled with N_2. **a** The logarithm of absolute impedance as a function of frequency logarithm. **b** The logarithm of phase shift as a function of frequency logarithm

600 times smaller than in the case of negligible deposition (Table 2). Besides the electrode reduction process, the change can be attributed to the formation of new Ni–Co solid-phase layers, which change the graphite electrode into a metallic electrode. The *CPE-T* value is quite small compared to the values in Table 2 and the slight increase with increasing suspension density is attributed to the increasing particle number, which increases the active surface. The addition of solid particles to the electrolyte at −900 mV means an enlargement of the working electrode surface. The probability of particle contacts with the electrode as well as mutual particle contacts also increases with the suspension density. Enlarging the electrode interface area leads to an increase in CPE and a decrease of R_C. The values of the Warburg impedance are nearly constant. They seem to describe the diffusion in the electrolyte perpendicular to the planar PIGE cathode surface. Then it is to be expected that these parameters are only dependent on the electrolyte concentration and thus must be constant in these experiments.

The Warburg impedance is a function of three parameters: $Z_W = f(W\text{-}T, W\text{-}R, W\text{-}P)$, where $W-R$ is the effective electrolyte resistance, $W-T$ is the diffusion time constant ($W-T = \delta^2 / D$, where D is the diffusion coefficient of the reduced species and δ is thickness of finite diffusion layer) and $W-P$ is the phase factor ($0 < W-P < 1$). The thickness of the diffusion layer δ (Table 3) was calculated assuming a value for the diffusion coefficients of $D = 1\times10^{-5}$ cm^2 s^{-1} for all species.

The results obtained by fitting were in good agreement with the measured data. The relative errors of most parameters (R_S, $W-T$, $W-R$ and $W-P$) were in the range of 0.7% to 2.6%. The highest errors were found for R_C, CPE-P and particularly for CPE-T. Increasing suspension density caused increase in the errors of these parameters. The relative errors of the circuit elements calculated from equivalent circuit model in Fig. 4b are presented in Table 4.

Conclusions

The electrochemical impedances were measured in order to investigate the charge transfer in fluidised bed arrangement. EIS experiments were performed during electrolytic coating of iron powder particles with binary Ni–Co layer. The effect of suspension density was studied.

The fluidised bed electrode behaviour at potential of 0 V was simulated with the equivalent circuit consisting of the electrolyte resistance, the constant phase element

Table 3 The values of equivalent circuit elements calculated from equivalent circuit model in Fig. 4b

Mass of Fe powder in 50 ml of electrolyte/g	R_S/Ω	W-R/Ω	W-T×10^7/s	W-P	R_C/Ω	$\delta\times10^6$/cm	CPE-T/m F	CPE-P
0	4.43	9.21	7.70	0.71	17.7	2.78	0.83	0.67
2	3.68	6.06	7.35	0.71	6.23	2.71	18.3	0.49
4	3.11	4.06	6.77	0.73	2.44	2.60	29.9	0.66
6	3.00	3.78	6.63	0.73	1.11	2.58	118	0.56
8	3.07	4.37	6.87	0.72	1.28	2.62	123	0.51
10	3.09	4.99	7.15	0.71	1.25	2.67	137	0.52
12	3.21	5.31	7.36	0.71	1.48	2.71	148	0.47

Table 4 The values of relative errors for values of equivalent circuit elements calculated from equivalent circuit model in Fig. 4b

Error/%	R_S	W-R	W-T	W-P	R_P	CPE-T	CPE-P
Electrolyte	2.24	1.33	1.17	0.78	1.11	8.47	1.84
2 g/50 mL	2.60	1.91	1.54	1.05	4.09	14.75	5.59
4 g/50 mL	1.81	1.52	1.15	0.81	3.60	16.12	5.31
6 g/50 mL	1.83	1.61	1.17	0.83	9.31	32.37	12.99
8 g/50 mL	1.88	1.50	1.15	0.81	9.97	31.16	13.38
10 g/50 mL	2.01	1.42	1.16	0.81	11.44	33.96	14.96
12 g/50 mL	2.17	1.54	1.27	0.88	13.68	34.72	16.67

and the charge-transfer resistance. The Warburg element was added in case of measurements at a potential of −900 mV.

The optimal suspension density for the charge transfer in the bed was observed in the range 10×10^{-3}–15×10^{-3} (i.e., 4–6 g of iron powder in 50 ml of electrolyte). First additions of iron particles into the electrolyte solution lowered the charge-transfer resistance. The conduction of the electric current through the dispersed phase of fluidised bed for such a low amount of powder particles was explained to be due to the convective mechanism.

It was found that iron particles dispersed in the electrolyte may act in two different ways: (1) as depolariser or (2) as supplementary working electrode. The role of iron particles in the studied heterogeneous system depends on the applied electrode potential and on the suspension density.

Further experiments are planned in order to investigate the influences of particle size, rotation speed, higher suspension densities, and applied DC potentials in detail. Moreover it is necessary to find a suitable mathematical model describing the hydrodynamic, granulometric and electrochemical parameters in the fluidised bed reactor and perhaps a more realistic equivalent circuit.

Acknowledgements This work was supported by the Slovak Grant Agency VEGA, projects No. 1/9038/02 and No. 1/2118/05.

References

1. Fleischmann M, Oldfield JW (1971) J Electroanal Chem 29:211
2. Held J, Gerischer H (1963) Ber Bunsenges Physik Chem 67:921
3. Sabacky BJ, Evans JW (1977) Metall Trans 8B:5
4. Yen SCH, Yao CHY (1991) J Electrochem Soc 138:2344
5. Gabrielli C, Huet F, Sahar A, Valentin GJ (1992) J Appl Electrochem 22:801
6. Gabrielli C, Huet F, Sahar A, Valentin GJ (1994) J Appl Electrochem 24:481
7. Shvab NA, Stefanjak NV, Kazdobin KA, Wragg AA (2000) J Appl Electrochem 30:1285
8. Shvab NA, Stefanjak NV, Kazdobin KA, Wragg AA (2000) J Appl Electrochem 30:1293
9. Fleischmann M, Oldfield JW (1971) J Electroanal Chem 29:231
10. Sabacky BJ, Evans JW (1979) J Electrochem Soc 126:1176
11. Lux L, Stašková R, Gálová M (1996) Acta Chim–models in Chemistry 133:115
12. Gálová M, Lux L, Oriňáková R (1998) J Solid State Electrochem 2:2
13. Lux L, Gálová M, Oriňáková R, Turoňová A (1998) Partic Sci Technol 16:135
14. Gál M, Gálová M, Turoňová A (2000) Collect Czech Chem Commun 65:1515
15. Lux L, Oriňáková R, Gálová M (1997) Acta Metallurgica Slovaca 3:603
16. Doherty T, Sunderland JG, Robersts EP, Pickett DJ (1996) Electrochim. Acta 41:519
17. Fouad MQ, Uzma B, Nuzhat A (2001) Appl Environ Microbiol 67:4349
18. Kongsricharoern N, Polprasert C (1995) Water Sci Technol 31:109
19. Tutovan V, Velican N (1971) Thin Solid Films 7:219
20. Kefalas JH (1966) J Appl Phys 3:37
21. Clauss RJ, Klein RW, Tremmel RA, Adamowicz NC (1971) American Electroplates Society, New York, pp 679
22. Brenner A (1963) Electrodeposition of alloys, principles and practice volume II. Academic, New York and London, pp 239
23. Golodnitsky D, Rosenberg Yu, Ulus A (2002) Electrochim Acta 47:2707
24. Fan Ch, Piront DL (1996) Electrochim Acta 41:1713
25. Sasaki KY, Talbot JB (2000) J Electrochem Soc 147:189
26. Bockris JOM, Drazic D, Despic AR (1961) Electrochim Acta 4:325
27. Allongue P, Cagnon L, Gomes C, Gündel A, Costa V (2004) Surf Sci 557:41
28. Bockris JOM, Reddy AKN (1970) Modern electrochemistry. Plenum, New York